Supporting Information for

Nanostructural Evolution and Self-Healing Mechanism of Micellar Hydrogels

Volkan Can[1], Zdravko Kochovski[2], Valentin Reiter[2], Nikolai Severin[2], Miriam Siebenbürger[1], Ben Kent[1], Justus Just[1], Jürgen P. Rabe[2], Matthias Ballauff[1,2], and Oguz Okay*[1,3]

[1]Helmholtz-Zentrum Berlin, Soft Matter and Functional Materials, Hahn-Meitner-Platz 1, D-14109 Berlin, Germany
[2]Humboldt-Universität zu Berlin, Department of Physics & IRIS Adlershof, Newtonstr. 15, D-12489 Berlin, Germany
[3]Istanbul Technical University, Department of Chemistry, 34469 Maslak, Istanbul, Turkey

Table of Contents

Experimental part

Materials. Deuterium oxide (D$_2$O, Aldrich), acrylamide (AAm, Merck), n-octadecylacrylate (C18A, Aldrich), N-isopropylacrylamide (NIPA, Sigma), sodium dodecylsulfate (SDS, Sigma), ammonium persulfate (APS, Merck), N,N,N',N'-tetramethylethylenediamine (TEMED, Merck), n-hexadecane (C16, Alfa Aeser) and NaCl (Merck) were used as received. Commercially available stearyl methacrylate (C18M, Fluka) used in the present work as the hydrophobic monomer consists of 65 % n-octadecyl methacrylate and 35 % n-hexadecyl methacrylate. An APS stock solution was prepared by dissolving 0.8 g APS in 10 mL of distilled water or in D$_2$O.

Preparation of micellar solutions and hydrogels. Various amounts of SDS were added to aqueous NaCl solutions at 35°C and then stirred for 4 h. The homogeneous micellar solutions were left at 35°C at least for one day before the rheological and DLS measurements. To investigate the effect of additives on the micellar structure, certain volume of the micellar solutions at 35°C was transferred into empty vials containing various amounts of AAm, NIPA, C16, C18A, and C18M and stirred at 35°C overnight. The solutions were left at 35°C for one day before the measurements. The solubilization extent of the hydrophobes in the micellar solution was estimated by measuring the transmittance of SDS-NaCl solutions containing various amounts of hydrophobes on a Agilent 8453 UV-visible spectrophotometer. The transmittance at 500 nm was plotted as a function of the added amount of the hydrophobe in the SDS-NaCl solution and, the solubilization extent was determined by the curve break. It was found that, for the concentration range studied, the hydrophobic monomers C18A and C18M are completely soluble in 243 mM SDS in 1 M NaCl solution while the solubility for C16 is 70 $\pm$ 10 mM.

For the preparation of hydrogels, C18M (26.3 mM) was first solubilized in 243 mM SDS - 1 M NaCl solution at 35°C and then, AAm (1.29 M) was added. The copolymerization reactions were conducted at 35°C in the presence of an APS (3.5 mM) - TEMED (0.25 v/v %) redox initiator system.

Rheological experiments. The measurements were carried out at 35$^\text{o}$C on an Anton Paar MR301 rheometer. The surfactant solutions of about 5 mL in volume were loaded into the sample chamber of a double-gap type geometry (C-DG 26.7/T200, internal diameter 23.833 mm, external diameter 27.594 mm, Anton Paar) equipped with a solvent trap to prevent the evaporation. The rheometer was connected to a circulating water bath (Viscotherm VT 2, Anton Paar), and the temperature was controlled with a Peltier system (Anton Paar) to maintain it constant at 35 °C with an accuracy of ± 0.1 °C. Zero-shear viscosities η_o were estimated by fitting the viscosity data to the Carreau model (Carreau, P. J. Trans. Soc. Rheol. 1972, 16, 99),

$$\eta(\dot\gamma) = \eta_o \left[1 + (\dot\gamma/\gamma_c)^2 \right]^{-n/2} \tag{S1}$$

where γ_c is the critical shear rate and n is the shear thinning index of the shear thinning region (Figure S1). The samples were also subjected to frequency sweep tests performed at a deformation amplitude γ_o = 0.01.

X-ray diffraction (XRD) measurements. XRD pattern were collected on a PANalytical X'Pert Pro diffractometer system equipped with Pixel-Array detector at a fixed divergence optic for incident beam in a Bragg-Brentano geometry, and a Cu-Kα source with nickel filter (λ = 0.15406 nm). Measurements are carried out at room temperature with sample and empty substrate for background subtraction between 1°- 19° 2θ range, with a scan rate of 0.5° / min.

Dynamic light scattering (DLS) experiments. DLS measurements were performed at 35$^\text{o}$C using ALV/ DLS/SLS-5000 compact goniometer (ALV, Langen, Germany) equipped with a He-Ne laser (λ = 632.8 nm). The temperature of the samples was controlled by a thermostat (Rotilabo, ±0.1 °C). The scattering angle θ was varied between 50 and 130$^\text{o}$ with steps of 10°. For solutions, the acquisition time for each run was 30 s. Intensity correlation functions of the hydrogels were acquired applying various measurement times between 30 s and 3h. The samples were filtered through Nylon membrane filters with a pore size of 0.2 μm into light scattering vials and tempered one day at 35$^\text{o}$C to assure

conformational equilibrium of the surfactant solutions. For ergodic media like surfactant solutions, the average intensity correlation function $g_T^{(2)}(q, \tau)$ can be written as the Laplace transform of the distribution of relaxation rates, $G(\Gamma)$:

$$g_T^{(2)}(q,\tau)-1 = \left[\int_0^\infty G(\Gamma)\exp(-\Gamma\tau)d\Gamma \right]^2 \tag{S2}$$

where τ is the decay time and Γ is the characteristic relaxation rate. $G(\Gamma)$ values at nine angles between 50° and 130° were evaluated with an inverse Laplace transform of ICF′s with the integrated ALV software. The relaxation rate of the fast mode Γ_{fast} was obtained from the peak values of Γ in $G(\Gamma)$s (Figures S2 and S3). Since for a diffusive process, the relaxation rate of a particular mode is q^2 dependent and is related to the diffusion coefficient as $\Gamma = D_A q^2$, the apparent diffusion coefficient D_A was calculated from the slope of Γ_{fast} vs q^2 plots (Figure S4). The hydrodynamic correlation length ξ_H on the basis of the fast mode was evaluated using the Stokes-Einstein relation, $\xi_H = RT/(6\pi\eta D_A)$, where η is the viscosity of the medium and kT is the Boltzmann energy.

Small-angle neutron scattering (SANS) measurements. SANS measurements were conducted at the time-of-flight SANS-beamline V16 at the Helmholtz Centrum Berlin. Two different q-range settings (setting 1: sample detector distance: 6.0 m; chopper speed: $\nu = 1200$ rpm; phase shift of chopper 3 and 4: $\phi_3 = 5^\circ$; $\phi_4 = 65^\circ$; setting 2: sample detector distance: 1.7 m; chopper speed: $\nu = 3000$ rpm; phase shift of chopper 3 and 4: $\phi_3 = 5^\circ$; $\phi_4 = 100^\circ$) were applied in order to cover a q-range between $q = 0.01 - 0.7$ Å^{-1}. The wavelength range is in between $\lambda = 1.8 - 6.9$ Å with $\Delta\lambda/\lambda \leq 10\%$ for both settings.

Cryo-electron microscopy. Cryo-electron microscopy (cryo-EM) specimens were prepared by vitrification of thin liquid films of the surfactant solutions supported on holey carbon-coated copper TEM grids (Quantifoil Micro Tools GmbH, Jena, Germany) in liquid ethane at its freezing point using a Vitrobot Mark IV (FEI, Eindhoven, Netherlands) set at 35°C and 95% humidity. The specimens were

inserted into a cryo transfer holder (Gatan 914, Gatan, Munich, Germany) and transferred into a JEOL JEM-2100 (JEOL GmbH, Eching, Germany) transmission electron microscope for imaging. Examinations were carried out at temperatures around 90 K. The TEM was operated at an acceleration voltage of 200 kV, and a defocus of the objective lens of about 3–5 μm was used to increase the contrast. All micrographs were recorded digitally with a bottom-mounted 4*4k CMOS camera (TemCam-F416, TVIPS, Gauting, Germany) at a magnification of 50 000x, corresponding to a pixel size of 2.32 Å at the specimen level. The total electron dose in each micrograph was kept below 20 e⁻/Å^2.

   Scanning force microscopy (SFM). The hydrogel samples for SFM measurements were prepared in the form of films by dipping microscope slides into a glass beaker filled with the gelation solution. Then, the slides were brought into a closed container at 35°C saturated with water vapor and the gelation reactions were conducted for one day. The slides were then transferred in SFM for the measurements. The imaging was performed with Nanowizard III (JPK Instruments AG) in Quantitative Imaging (QI) mode and with commercial N-doped silicon cantilevers (OMCL-AC240TSG-R3, resonant frequency 70 kHz, spring constant 2 N/m, Olympus Corporation). For cutting of gels, SFM instrument was operated in contact mode, the tip was moved at a constant speed between 0.1 to 1 μm/s along a designed path pushing onto the surface with typical forces between 1 and 10 nN. We did not calibrate cantilever sensitivity by pushing it onto a hard surface to avoid possible tip apex damage, but instead we assumed the cantilever spring constant to be 2 N/m and adjusted the sensitivity within the thermal tuning method to obtain the assumed spring constant. The SFM instrument was located inside an acoustic isolation box. Temperature and relative humidity (RH) inside the box were increased by heating up a petri dish filled with water (deionized and purified water, Protegra CS Systems CEDI Technology >10. MΩ·cm). RH and temperatures were measured with a sensor (testo 635 and testo 625 of Testo GmbH) located in a close proximity of the SFM head. The calibration fidelity of the sensors is ±2.5% RH in the addressed RH range, as provided by the manufacturing company. RH values indicated in the text are the displayed

values. The images were processed with either JPK data processing software or SPIP (Image Metrology). Topography images were line flattened with polynomials of 1st or 2nd order with substantial corrugations manually excluded from line fitting.
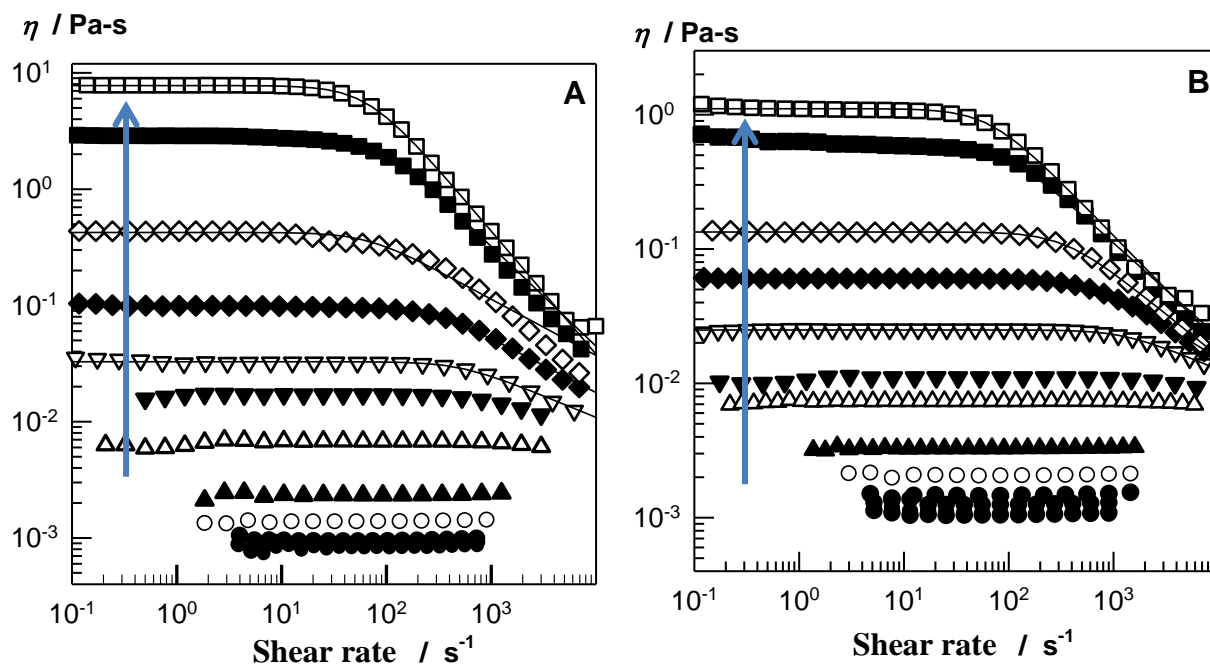

Fig. S1. Shear rate $\dot{\gamma}$ dependence of the viscosities η of aqueous SDS – NaCl solutions at 35°C. The arrows indicate increasing SDS (A) and NaCl concentrations (B). The curves are the best fits of the data to the Carreau model (see Supplementary Text). **A:** NaCl = 1M. SDS = 0 - 20 (●), 35 (○), 59 (▲), 104 (△), 142 (▼), 173 (▽), 243 (◆), 347 (◇), 520 (■), and 693 mM (□). **B:** SDS = 243 mM. NaCl = 0 – 0.50 (●), 0.60 (○), 0.67 (▲), 0.74 (△), 0.80 (▼), 0.87 (▽), 0.94 (◆), 1.0 (◇), 1.2 (■), and 1.3 M (□).
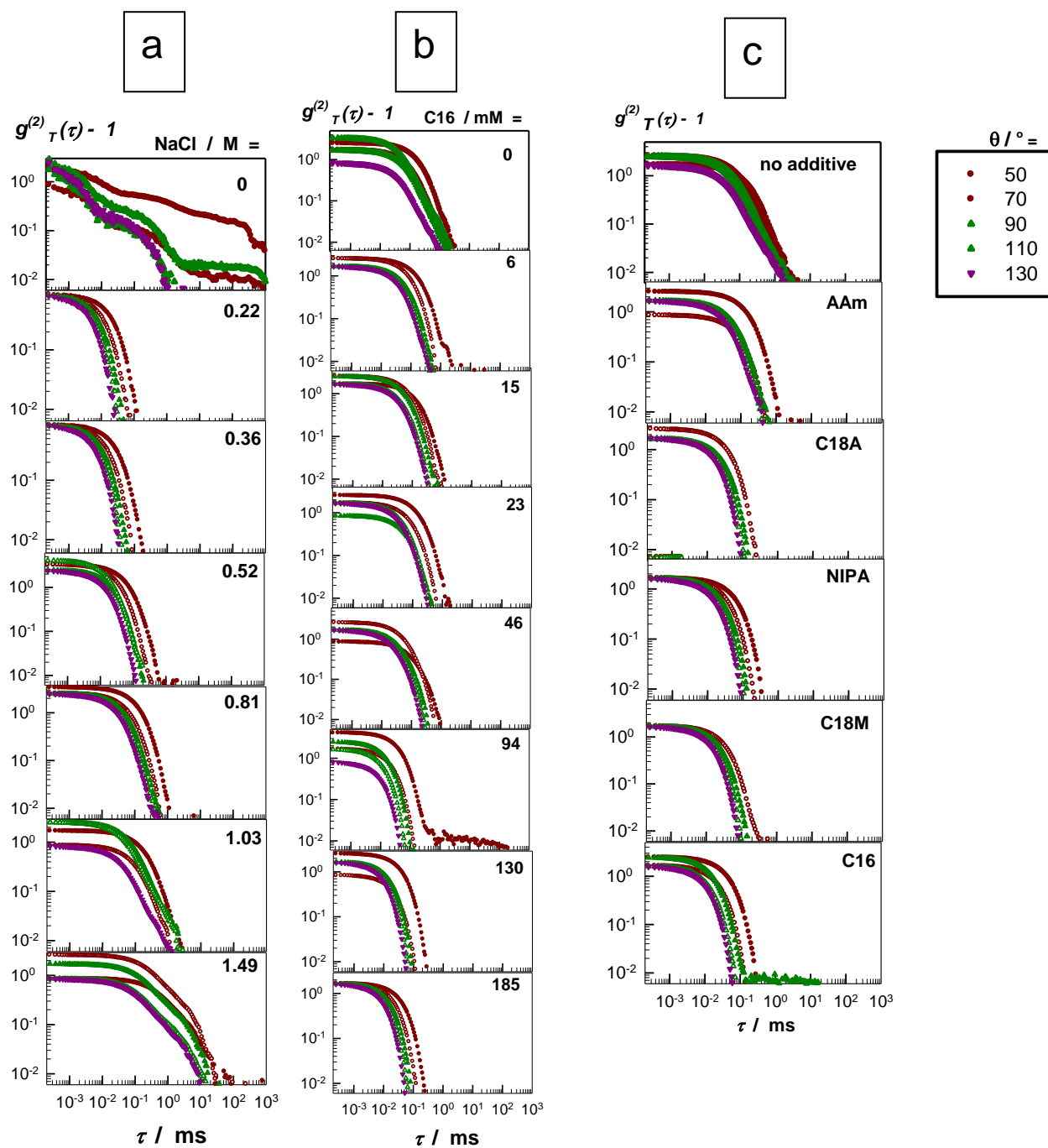
Fig. S2. The time average intensity correlation functions ICFs ($g^{(2)}_T(\tau) - 1$)) at five scattering angles θ between 50° and 130° of 243 mM SDS solutions at 35°C. Solutions containing various amounts of NaCl (a), of n-hexadecane C16 at 1 M NaCl (b), and various types of additives (130 mM) at 1 M NaCl (c).
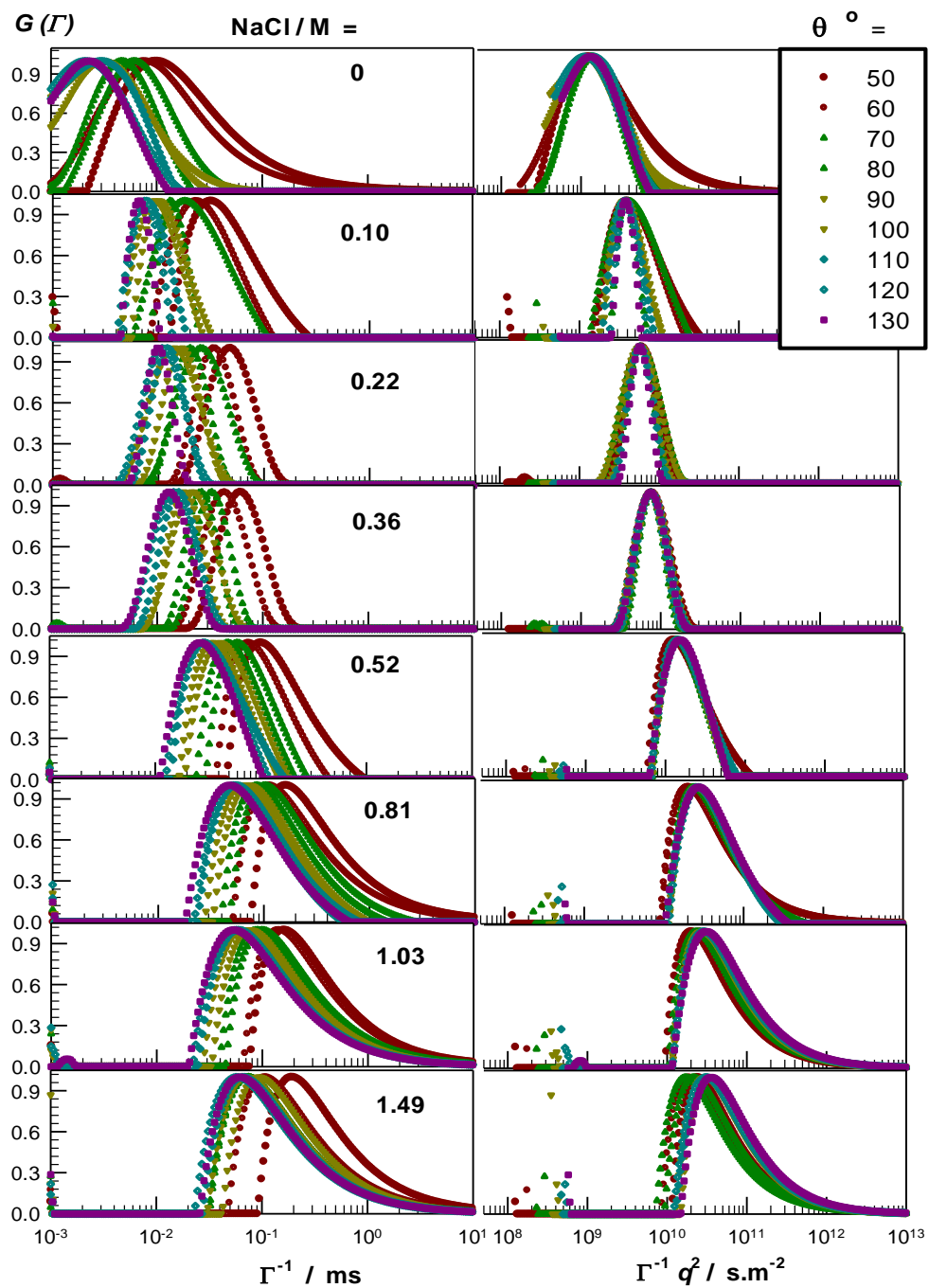
Fig. S3a. $G(\Gamma)$ vs Γ^{-1} (left) and $\Gamma^{-1}q^2$ plots (right) at various angles θ for 243 mM SDS in aqueous NaCl solutions of various concentrations indicated (in M). Temperature = 35°C.
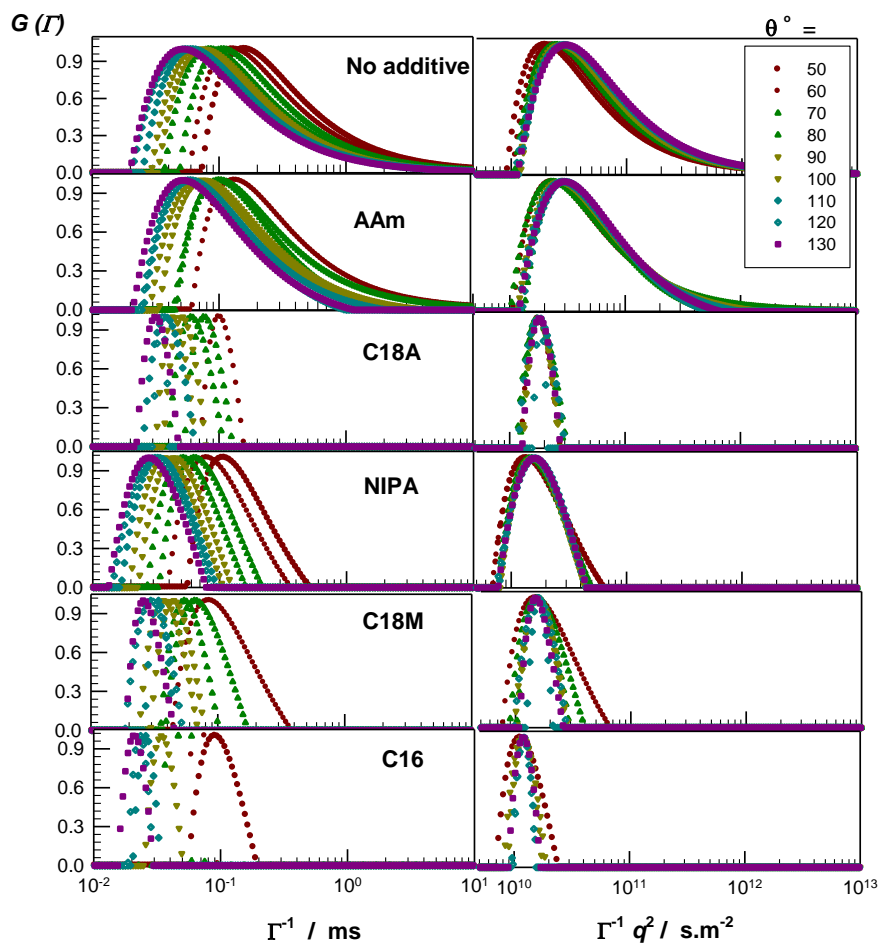
Fig. S3b. $G(\Gamma)$ vs Γ^{-1} (left) and $\Gamma^{-1}q^2$ plots (right) at various angles θ for 243 mM SDS in 1M NaCl solutions and in the presence of 130 mM additives indicated. Temperature = 35°C.
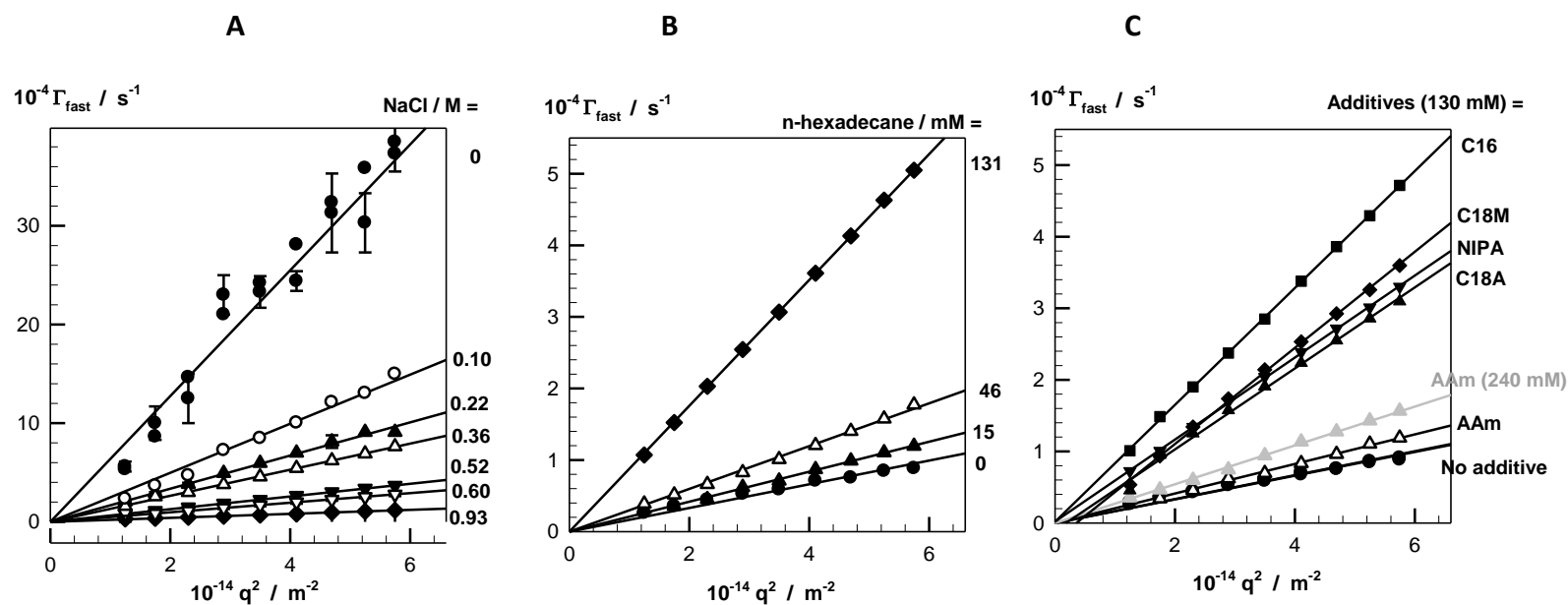
Fig. S4. Relaxation rate of the fast mode Γ_{fast} plotted against q^2 for surfactant solutions.
A: 243 mM SDS in NaCl solutions of various concentrations as indicated (in M).
B: 243 mM SDS in 1M NaCl solution in the presence of various amounts of n-hexadecane as indicated.
C: 243 mM SDS in 1M NaCl solution in the presence of various additives at a concentration of 130 mM.
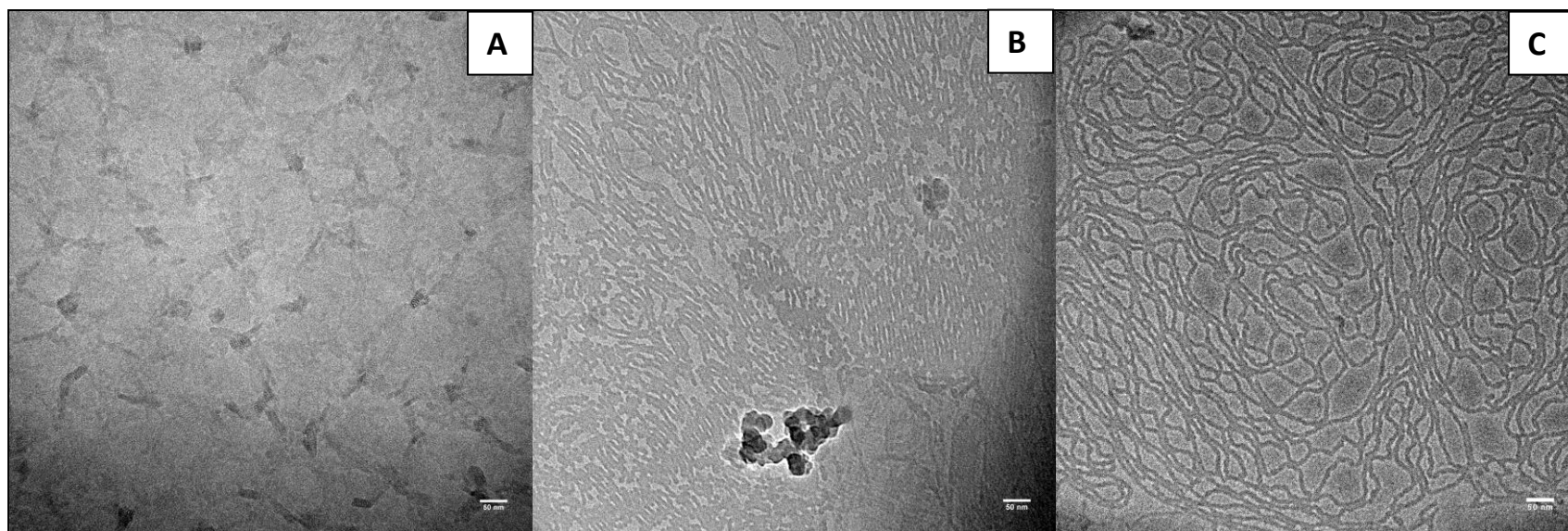
Fig. S5. Cryo-EM micrographs of surfactant solutions. 243 mM SDS in 1 M NaCl solution before (A) and after 1:5 (B) and 1:10 dilutions with 1 M NaCl (C). Scale bars = 50 nm.
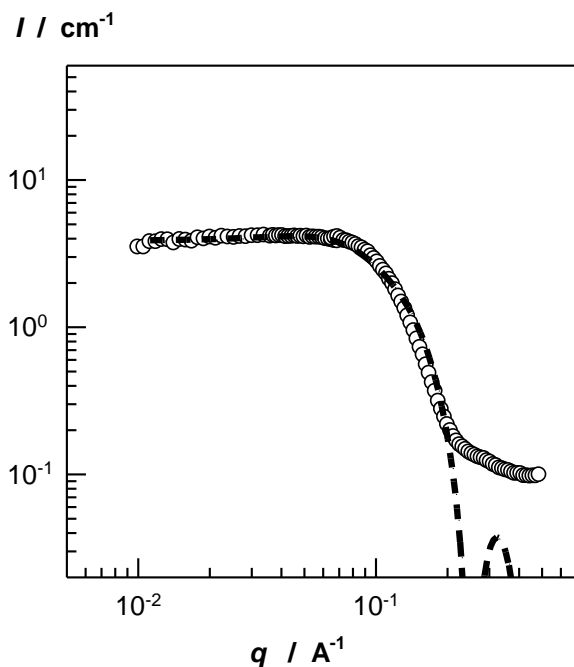
Fig. S6. SANS profile for 243 mM SDS in 1 M NaCl solution after addition of 1.29 M AAm. The dashed curve is best fit to a form factor of spheres with a radius of 1.8 nm.
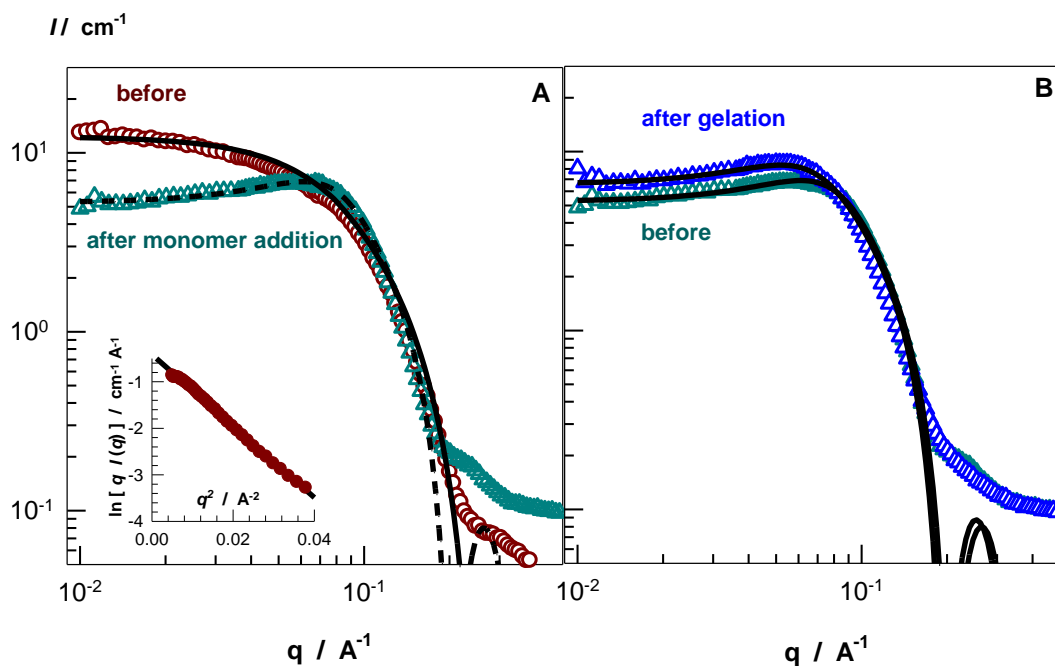

Fig. S7. (A): SANS profiles for 243 mM SDS in 0.5 M NaCl solution before and after monomer addition. The solid and dashed curves are best fits to a form factor of wormlike micelles and spheres, respectively. The inset shows $\ln [I(q) q]$ vs q^2 plot for the solution before the addition of monomers in the range of $q = 0.06 - 0.19$ A^{-1}. (B): SANS profiles for 243 mM SDS in 0.5 M NaCl solution containing the monomers AAm (1.29 M) and C18M (26.3 mM). The samples were measured before and after gelation. The curves are best fits to a form factor of spheres with a radius of 2.2 nm (before gelation) and 2.3 nm (after gelation).
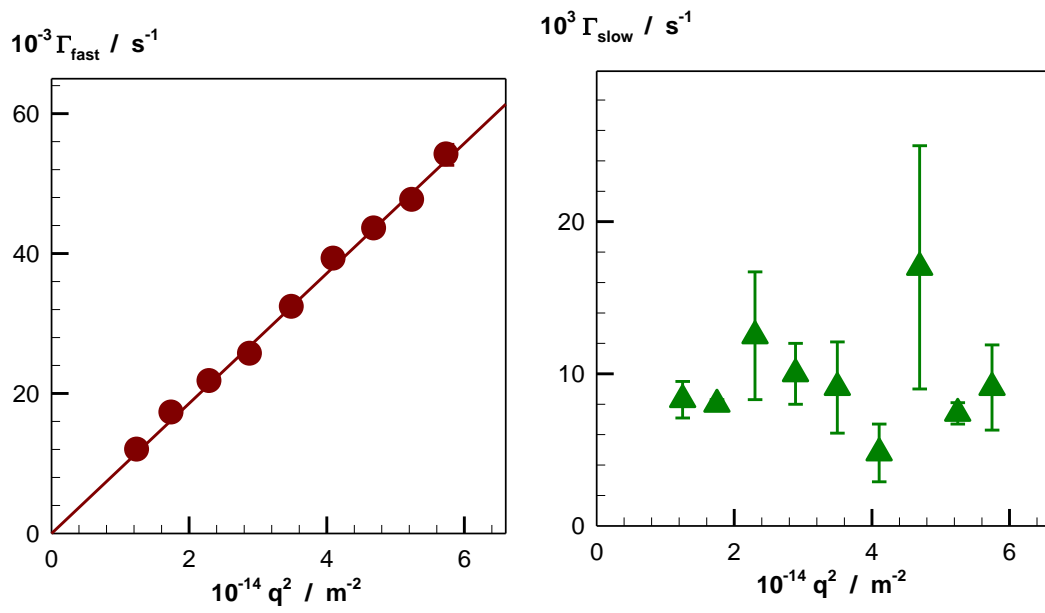
Fig. S8. Relaxation rates of the fast (Γ_{fast}) and slow modes (Γ_{slow}) plotted against q^2 for the hydrogels. ICFs were obtained at an acquisition time of 1000s.
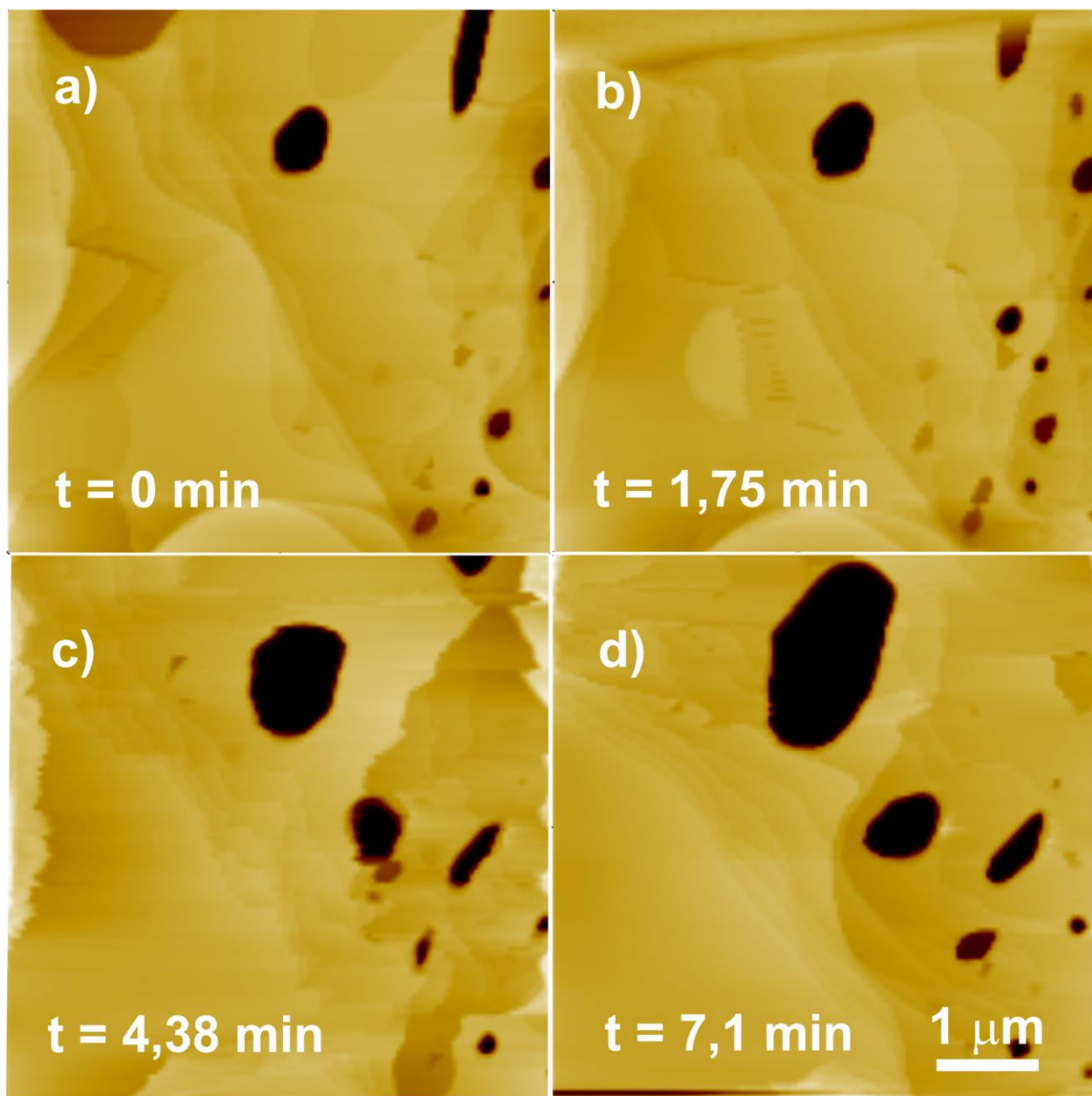
Fig. S9. Topography images successively taken in the same location. The imaging was performed at the elevated temperature and humidity as indicated in the text. The topography shows terraces and holes that continuously reshape. The color scale form black to white of the images is 200 nm.
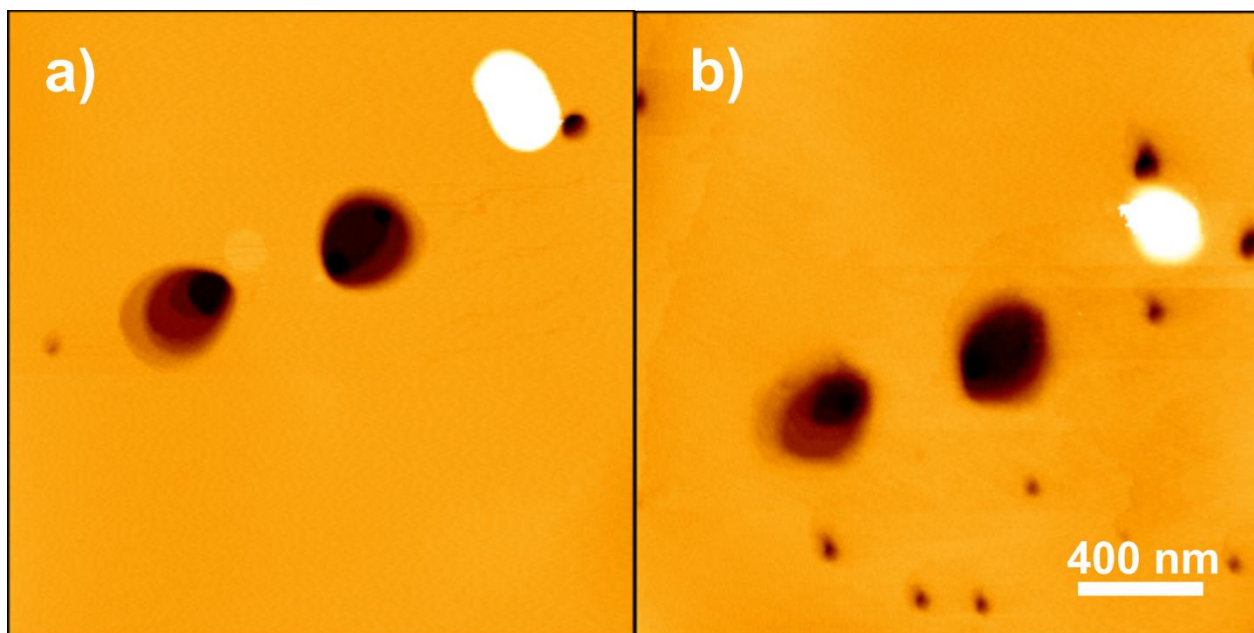
Fig. S10. a) Topography of gel surface imaged after 1.5 h of gel cutting. The cut relaxed to holes and the relaxation is demonstrated in Figure S11b. **b)** Topography of the same spot imaged after 18 h of sample resting under ambient condition. A few small holes appeared in addition to the initial ones. This can be a result of gel drying at ambient. The color scale of the images is 100 nm from black to white.
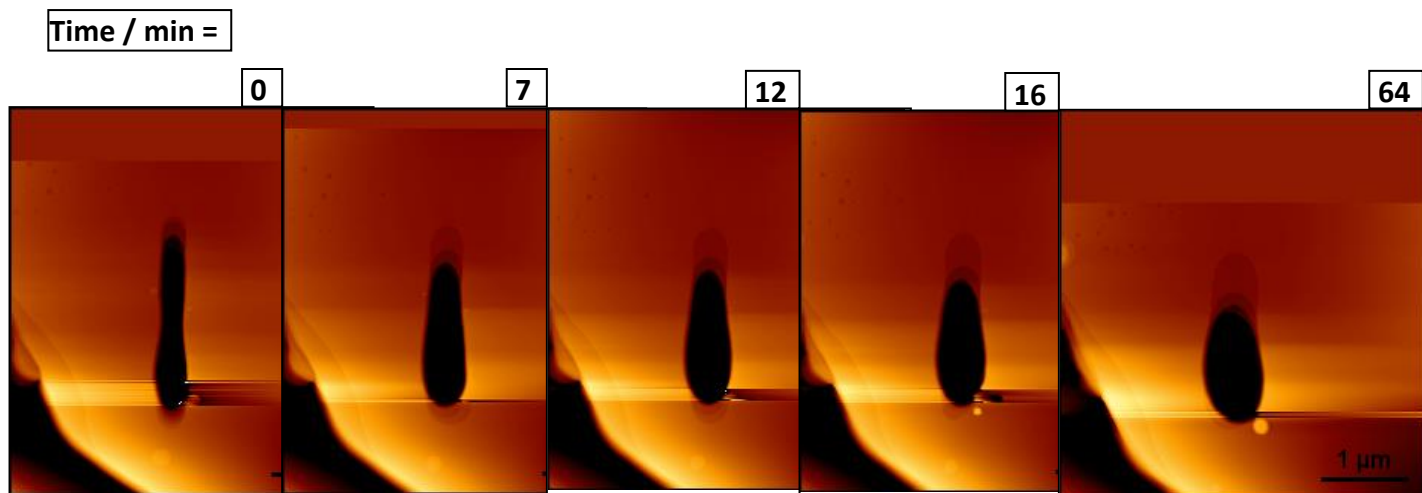
Figure S11a: Topographies of the gel surface imaged just after cutting (0), and after certain time elapsed as indicated.
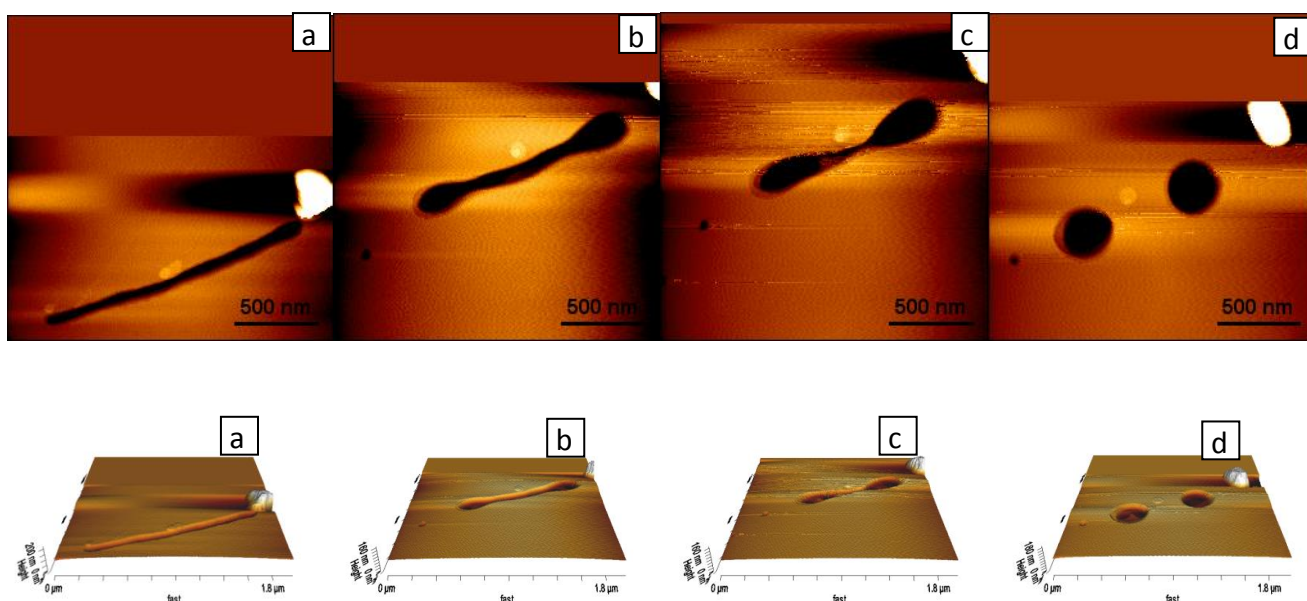

Figure S11b: Topographies of the gel surface imaged just after cutting and after certain time elapsed as indicated below. Initially elongated cut becomes first dumbbell-like and eventually relaxes into two circular holes. Imaging was performed under ambient conditions.

a) Initial cut: length = 1.6 μm, width = 100 nm, depth = 30-40 nm.

b) After 35 min: length = 1.3 μm, width = 120-130 nm capped with ellipsoidal holes 220-240 nm in width, depth = 30-40 nm.

c) After 40 min: length = 1.1 μm, width = 90-100 nm capped with ellipsoidal holes 210-260 nm in width, depth = 10 nm and 20-40 nm for the middle and end caps of the cut, respectively.

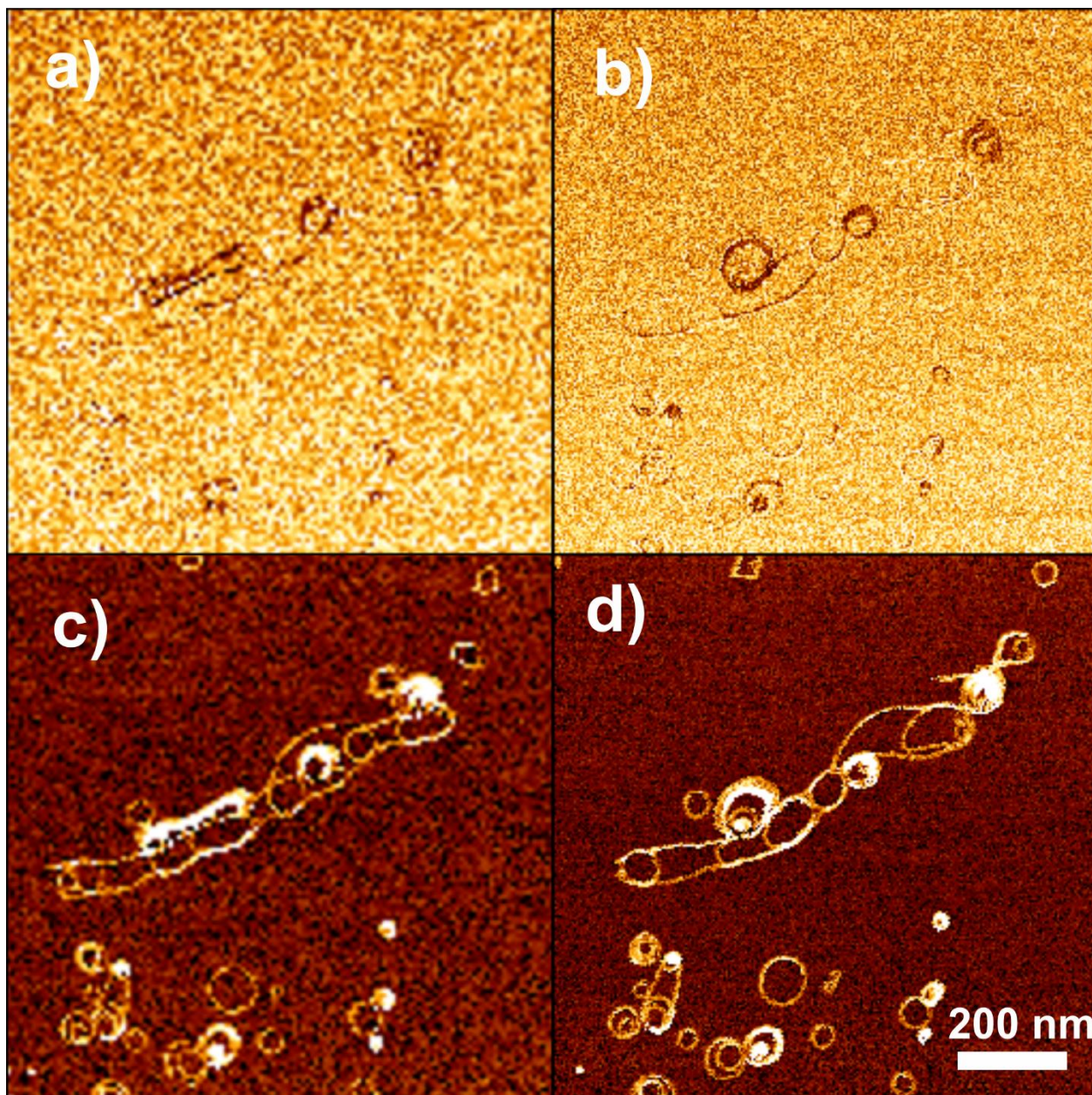d) After 50 min: Circular holes 300-400 nm in diameter, depth = 40 nm.

Fig. S12. Images of the force-distance extension curve slopes acquired simultaneously with the topography images demonstrated in a) Figure S10a and b) Figure S10b. The color scale from black to white of a) and b) is 1 N/m. Adhesion force images taken simultaneously with topography images demonstrated in c) Figure S10a and d) Figure S10b. The black to white color scale of c) and d) is 1.5 nN. No recognizable contrast between the virgin gel surface, bottoms of the trenches, and tops of the islands indicates that they have the same mechanical properties. The contrast along the edges can be explained with an SFM artifact, due to the tip sides being in contact with the sample and not the tip apex.